An Efficient and Accurate Way of Posing Inflow Profile Boundary Conditions

張　剣波，日産自動車（株）総合研究所，横須賀市夏島町１番地，j-zhang@mail.nissan.co.jp
森下　悦生，東京大学大学院，航空宇宙専攻，morisita@meyer.t.u-tokyo.ac.jp
Jianbo Zhang, Nissan Motors, Co. LTD. , 1, Natsushima-cho, Yokosuka-shi
Etsuo Morishita, The University of Tokyo, 7-3-1, Hongo, Bunkyo-ku, Tokyo

An efficient and highly accurate way to systematically reproduced the inflow boundary profiles for the mean flow variables, as well as the turbulent quantities in one-equation and two-equation turbulence-models, from given external flow conditions and one boundary layer parameter, is described. The reproduced profiles are checked against both experimental results and numerical solution of boundary layer equations. Theoretical analysis shows that a new form of density-weighted velocity, rather the Van Driest density-weighted velocity, obeys the linear-law at the viscous sublayer in a compressible turbulent boundary layer. Especially for nonadiabatic wall at hypersonic Mach numbers, where there are large density gradients, these two kinds of density-weighted velocity could differ considerably. It is also shown that power-law fitting for the streamwise velocity gives unacceptable profile in the viscous sublayer. For first time, an efficient way to specify the normal velocity profile is proposed and tested. The reproduced normal velocity at boundary layer edge is found to agree remarkably well with numerical solution of boundary layer equations.

Nomenclature

a_e = sound speed at boundary layer edge
c_f = local skin-friction coefficient, $t_w/(r_e u_e^2/2)$
c_p = specific heat at constant pressure
H = shape factor or intermediate variable in Eq. (7)
k = turbulent kinetic energy per unit mass
L_{ref} = reference length scale
M = Mach number
n =exponent in the power-law for molecular viscosity
N =exponent in the power-law fit for streamwise velocity
P = pressure
Pr_t = turbulent Prandtl number, 0.9
q = heat flux
$Re|m$ = unit Reynolds number per meter
Re_q = Reynolds number based on momentum thickness, $r_e u_e q/m_e$
Re_{d2} = empirically-chosen Reynolds number, based on viscosity at the wall, $r_e u_e q/m_w$
T = temperature
u = Farve-averaged streamwise velocity
u^+ = u/u_t
u_t = friction velocity, $(\tau_w/\rho_w)^{1/2}$
u_c = transformed velocity according to Eq. (2) or (10)
v = Farve-averaged normal velocity
x = streamwise coordinate
y = distance above the wall
y^+ = yu_t/n_w
Dx = streamwise integration step
e = dissipation rate
η = y/d
d = boundary layer nominal thickness
d^* = displacement thickness
P = profile parameter in Coles' formula
q = momentum thickness
m = molecular viscosity
m_t = turbulent eddy viscosity
n = kinematic viscosity
$\tilde{n}$ = modeled quantity in Spalart-Allmaras's turbulence model
r = mass density
t = shear stress
t_{xy} = principal turbulent shear stress
ω = specific dissipation rate

Subscripts

0 = stagnation condition
e = boundary layer edge
w = wall

Abbreviation

CFD = computational fluid dynamics
BL = boundary layer

1. Introduction

Much of research efforts in CFD have been devoted to the grid generation, discretization of the governing equations, and the solution of the resultant system of algebraic equations. Attention has also been paid to the posing of appropriate numerical boundary conditions around the solution domain. While the treatment of boundary conditions at nearly uniform inflow, wall, farfield, and outflow[1-5] has reached a high degree of sophistication, the specification of solution variables across compressible turbulent boundary layer at inflow is rather crude. Common practice simply uses the power-law for streamwise velocity, with the exponent fitted from experimental results. The temperature profile is obtained via Crocco integral, and the density profile through equation of state with the assumption of constant pressure across the boundary layer. Empirical formulas, simulating typical profiles in a boundary layer, for the turbulence kinetic energy, turbulence dissipation rate and specific dissipation rate are employed in CFL3D[6]. Zero normal velocity is usually assumed for convenience. However, it is demonstrated[7] the zero normal velocity assumption would lead to spurious expansion and compression waves near the inflow region.

One reason why people are not much disturbed by such crude treatment is the hope that turbulent boundary layer would eventually develop to the equilibrium state by itself at some distance downstream. While this might be the case, it nonetheless requires extra length to be included in the inflow region of the solution domain. And it is not clear how long this development region should be. To reduce the size of the solution domain and thereby reducing the computational overhead, numerical solutions of boundary layer equations at the station that matches the integral parameters from experiment is used by Zhang[8] as the inflow boundary conditions. This approach, while being highly accurate, is not quite efficient.

In this paper, based on the works in Ref. 9, an efficient and accurate way to systematically specify the inflow profiles for the mean flow variables, as well as the turbulent quantities in one-equation and two-equation turbulence-models, will be described. Theoretical analysis will show that a new form of

density-weighted velocity, rather than the Van Driest density-weighted velocity, obeys the linear-law in the viscous sublayer for high-speed flows. It will also be shown that power-law fitted stream-wise velocity distribution is unacceptable in the viscous sublayer. In addition, for the first time to the authors' knowledge, a way to specify the normal velocity profile will be proposed and tested.

2. Specification of Major Mean Flow Profiles

A number of theories[10-18] has been developed to determine skin-friction and specify velocity profile for compressible turbulent boundary layers. The general consensus is that the Van Driest I transformation[12] is a good fit to the experimental data of the velocity profile in the inner layer, and the Van Driest II transformation[17] offers a good fit to the experimental data of skin friction. Two limitations of Van Driest I transformation are that it is only valid for the log-law region and for turbulence Prandtl number (Pr_t) equal to one. The velocity profile of Huang et. al[16] is an extension of the Van Driest I transformation applied to Coles' profile[11] that includes the sublayer and the wake regions, and the transformation is modified to be valid for Pr_t equal to 0.9. This profile family is a good fit to the boundary layer velocity profiles for a wide range of Mach and Reynolds numbers. For completeness, the procedure proposed by Huang et. al. will be briefly described first. Its modifications and extensions by the present authors are then followed.

Experimental evidence[19] and theoretical analysis[12] suggest that the law-of-the-wall and the law-of-the-wake are transferable from incompressible flow to the compressible flow, provided that the velocity is defined by the density-weighted transformation and the wake parameter is correlated with empirically-chosen Reynolds number Re_{d2}. The law-of-the-wall for the inner region, including the linear-law region, the buffer region and the log-law region, combined with Coles' law-of-the-wake for the outer region reads:

$$u_c^+ = \frac{u_c}{u_t} = u_{c,b}^+ + \frac{\Pi}{k} w\left(\frac{y}{d}\right) \tag{1}$$

where

$$u_c = \int \left(\frac{r}{r_w}\right)^{1/2} du \tag{2}$$

and $u_{c,b}^+$ is a pure law-of-the-wall profile defined by

$$\frac{du_{c,b}^+}{dy^+} = \frac{2}{(1+4l^{+2})^{1/2}+1} \tag{3}$$

where

$$l^+ = ky^+(1-e^{-y^+/A^+}), \quad k \approx 0.41, \qquad A^+ = 25.53$$

The wake parameter P can be obtained from the curve fitting formula due to Cebeci and Smith[20]:

$$\Pi = 0.55[1-\exp(-0.24\sqrt{\mathrm{Re}_q} - 0.298\,\mathrm{Re}_q)] \tag{4}$$

As the pressure is nearly constant across the boundary layer, the density ratio in Eq. (2) can be replaced by temperature ratio, which can be obtained by neglecting the convection terms and integrating the energy equation near a solid surface,

$$T = T_w - \frac{Pr_t q_w u}{c_p t_w} - \frac{Pr_t u^2}{2c_p} \tag{5}$$

The above equation establishes the relationship between T_w and q_w/τ_w.

The integration of Eq. (2) yield the Van Driest transformation

$$u_c = \sqrt{B}\left[\sin^{-1}\left(\frac{A+u}{D}\right) - \sin^{-1}\left(\frac{A}{D}\right)\right] \tag{6}$$

where

$$A = q_w / t_w$$
$$B = 2c_p T_w / Pr_t$$
$$D = \sqrt{A^2 + B}$$

The inverse of Eq. (6) is

$$\frac{u}{u_t} = \frac{1}{R}\sin\left(\frac{Ru_c}{u_t}\right) - H\left[1-\cos\left(\frac{Ru_c}{u_t}\right)\right] \tag{7}$$

where

$$R = u_t / \sqrt{B}$$
$$H = A/u_t$$

To obtain c_f and the corresponding boundary layer profiles for a given boundary layer displacement thickness or momentum thickness, the following iterative procedure needs to be performed:

1) Given d^* (or q), guess d^*/d, q/d and u_t (or q/d and u_t).
2) Calculate $Re_{d2} = r_e u_e q/m_w$ and find P from Eq. (4).
3) Calculate $y_d^+ = u_t d/n_w$ and obtain $u_{c,d}^+$ from Eq. (1).
4) Obtain the nontransformed dimensionless velocity u_d^+ from Eq. (7).
5) Update $u_t = u_e/u_d^+$ and solve for $c_f = 2(T_e/T_w)(u_t/u_e)^2$.
6) Tabulate u as a function of $h=y/d$ using Eqs. (1) and (7).
7) Update d^*/d, q/d (or q/d^*) by performing the following integration numerically:

$$\frac{q}{d} = \int_0^1 \frac{ru}{r_e u_e}\left(1-\frac{u}{u_e}\right)dh$$

$$\frac{d^*}{d} = \int_0^1 \left(1-\frac{ru}{r_e u_e}\right)dh$$

where r/r_e is replaced by T_e/T with T obtained from Eq. (5).

Steps 1 to 7 are repeated until the solution converges.

Three modifications to the above procedure are proposed to make it more convenient and more accurate.

A. Explicit expression for the wall velocity distribution due to Musker[21]

Eq. (1) involves integration and is not convenient to use. In addition, there is a discrepancy in the slope condition at the edge of the boundary layer, as discussed by Cornish[22], Bull[23], and others. Instead, Musker's explicit expression for the law-of-the-wall at inner region and law-of-the-wake at outer region, satisfying the four boundary conditions: $y=0$, $u_c=0$ and $du_c^+/dy^+=1$; $y = d$, $u_c = u_{ce}$, and $du_c/dy = 0$, can be used to facilitate the iterative procedure.

$$u_c^+ = 5.424\tan^{-1}\left[\frac{2y^+-8.15}{16.7}\right] + \log_{10}\left[\frac{(y^+ +10.6)^{9.6}}{(y^{+2}-8.15y^+ +86)^2}\right] \tag{8}$$
$$-3.52 + 2.44\left\{\Pi\left[6\left(\frac{y}{d}\right)^2 - 4\left(\frac{y}{d}\right)^3\right] + \left(\frac{y}{d}\right)^2\left(1-\frac{y}{d}\right)\right\}$$

B. The velocity distribution at the viscous sublayer

Velocity distribution at the viscous sublayer for compressible turbulent boundary layer needs further examination. In Coles' original proposal for Eq. (1), the viscous sublayer is neglected. Huang et. al.[16] found that it is important to include the sublayer contribution for high-speed flows because the sublayer becomes thicker and may occupy a substantial portion of the whole boundary layer at hypersonic Mach number. In using Eq.

(1) as the base for their profile family, it is actually assumed that Van Driest transformed velocity, Eq. (2), obeys the same linear-law as that in the incompressible case. They acknowledge that they cannot claim detailed reliability of their profile family in the sublayer. As sublayer data for compressible flows are scarce, especially for large heat transfer rates, theoretical analysis will be pursued to examine this problem in the following.

As in the incompressible turbulent boundary layer, there is a thin layer of constant total shear stress, called the inner layer, in compressible turbulent boundary layer. In the turbulent core region, the laminar shear stress is dominated by the Reynolds stress and hence can be neglected. By assuming Pr_t equal to one and invoking Prandtl's mixing length theory, Van Driest[12] showed that the transformed velocity obeys the same log-law as that in the incompressible case. In the immediate vicinity of wall, due to the damping of the wall, Reynolds stress can be neglected. The laminar shear stress equals to the shear stress at wall:

$$m\frac{\partial u}{\partial y} = t_w$$

Divided with viscosity at wall, it becomes:

$$\frac{m}{m_w}\frac{\partial u}{\partial y} = \frac{r_w u_t^{\,2}}{m_w}$$

Integrating and using power-law for molecular viscosity:

$$\frac{\int\left(\frac{T}{T_w}\right)^n du}{u_t} = y^+ \qquad (9)$$

As before, the temperature ratio in Eq. (9) can be replaced by the density ratio:

$$\frac{\int\left(\frac{r}{r_w}\right)^{-n} du}{u_t} = y^+ \qquad (10)$$

It indicates that the velocity transformed according to Eq. (9) or (10) rather than Eq. (2) obeys the linear-law for high-speed flows. For adiabatic wall, the temperature, hence the density, is nearly constant in the viscous sublayer, therefore, these two kinds of transformation give essentially the same results. However, for non-adiabatic wall, especially for large heat transfer at hypersonic Mach number, large density gradient exists at the sublayer. These two kinds of transformation can be quite different. Therefore, for non-adiabatic wall, Eq. (9) or (10) should be invoked to modify the streamwise velocity after obtaining u_t through the iterative procedure described above. For a more accurate streamwise velocity distribution, Sutherland's law for molecular viscosity can be used instead of the power law in Eq. (9).

The actual calculation consists of the following three steps.

1) Determine u_t through the iterative procedure.
2) Substitute the Crocco's integral, Eq. (5), into Eq. (9), integrate it numerically, thereby establish y as a tabulated function of u.
3) Interpolate this tabulated function to find u at the desired value of y.

C. Reproduce velocity distribution from boundary layer thickness d

In the situation where the boundary layer thickness d is known or provided, rather than d^* or q, the following five steps could replace the first five steps in Huang's algorithm:

1) Given d, guess q and u_t, and calculate t_w.
2) Calculate u_{ce} from Eq. (6), calculate $Re_{d2} = r_e u_e q/m_w$ and find P from Eq. (4).
3) Calculate $Re_{d,w} = r_w u_{ce} d/m_w$.
4) Solve for y_d^+ from $Re_{d,w} = (u_{ce}/u_t)(r_w u_t d/m_w) = u_{cd}^+ y_d^+$ and Eq. (8).
5) Update $u_t = y_d^+ m_w/(r_w d)$, and solve for $c_f = 2(T_e/T_w)(u_t/u_e)^2$.

To test the effectiveness of these modifications in reproducing the compressible turbulent boundary layer profiles, the experimental results in Ref. 18 is chosen as benchmark. The external flow conditions are as follows:

$$M_e = 7.80, \quad Re|_m = 24.05\times10^6\, m^{-1}, \quad P_e = 1230\, Pa,$$
$$T_0 = 688\, K \quad T_w = 306\, K$$

Fig. 1 compares the streamwise velocity profiles reproduced from given q or d against that measured from experiment. The reproduced c_f, d or q are compared with the experimental results in Table 1.

Fig. 2 shows the reproduced density and temperature profiles across the boundary layer. It has to be noted that any usage of Crocco's integral, even with the inclusion of recovery factor to take into account the realistic turbulent Prandtl number, implies that velocity boundary layer thickness equal to temperature boundary layer thickness, which is not true for compressible flows, especially for hypersonic flows.

Fig. 3 compares the streamwise velocity distribution, in wall unit, in the viscous sublayer. The solid line depicts the streamwise velocity distribution according to Eq. (10), while the dashed curve depicts the same distribution but transformed according to Eq. (2). It is clear that difference of about 10% at the outer edge of viscous sublayer (y^+=5) exists between the two transformations. Although the distribution according to Van Driest transformation still closely resembles a straight line, the slope is quite different from that in incompressible case.

As noted in the introduction, it is common practice in experiment to fit velocity distribution across the boundary layer to power functions. In CFD, power-law velocity distribution is often used as a convenience to set the inflow streamwise velocity profile. However, it has to be pointed out that power-law is only approximately applicable to the outer part of the boundary layer. In the immediate vicinity of the wall, power-law assumption will result in qualitatively incorrect velocity distribution. In fact, at the wall, the normal derivative of streamwise velocity according to the power-law is singular. Two-equation turbulence models usually require the y^+ at the first grid point be less than 1, and there should be several grid points within the viscous sublayer, if wall-function approach is not used. In such a situation, the streamwise velocity distribution near the wall should be determined through the iterative procedure described above, rather than using power-law fitting. Fig. 4 compares the velocity distributions in sublayer, in wall unit, obtained from experimentally fitted power-law and that reproduced from the law-of-the-wall as analyzed in the subsection **B**. It is clear that the distribution obtained from the power-law is totally unacceptable in the viscous sublayer.

3. Specification of Normal Velocity Profile

Normal velocity within boundary layer is deemed sufficiently small and usually assumed to be zero for convenience. However, Orkwis et. al.[7] demonstrate in the simulation of consecutive flat plates that spurious shock and expansion waves will be generated as a result of zero normal velocity assumption in the inflow profile for the second plate. To the authors' limited knowledge, there has been no efficient way of specifying normal velocity profile for compressible

turbulent boundary layer in open literature. In this paper, by incorporating continuity equation and integral momentum equation with the iterative procedure in section II, a way to determine normal velocity profile is proposed and tested against boundary layer solution.

The Farve-averaged[24] continuity equation for steady compressible flow reads

$$\frac{\partial ru}{\partial x}+\frac{\partial rv}{\partial y}=0 \tag{11}$$

It follows that if the density and streamwise velocity profile at two closely located stations are known, the normal velocity profile can be obtained through the integration of Eq. (11). It is already shown in section II that the density and streamwise velocity profile at a station can be efficiently reproduced, with good accuracy, as long as the external flow conditions and one boundary layer parameter at that station are provided. The question left is how to find the density and streamwise velocity profile at the next station. For this purpose, momentum integral equation for a boundary layer over flat plate under zero-pressure gradient can be employed.

$$\frac{dq}{dx}=\frac{c_f}{2} \tag{12}$$

The procedure to specify normal velocity profile consists of the following steps:

1) Given the external flow conditions and one integral parameter, say, boundary layer momentum thickness q at one station, calculate the density, streamwise velocity profile, and skin friction coefficient c_f at that station through the algorithm described in section II.
2) Determine the boundary layer momentum thickness at the next station through the integration of Eq. (12).
3) Calculate the density, streamwise velocity profile at the new station in the same manner as in step 1.
4) Determine the normal velocity profile through the integration of Eq. (11).

To check the effectiveness of the above procedure, the sonic flow over an isothermal flat plate, employed by Wilcox[25] to instruct the usage of his boundary layer solution program EDDYBL, is chosen as benchmark. The external flow conditions are as follows:

$$M_e=1.0,\quad Re|_m=4.07\times10^6 m^{-1},$$
$$P_0=23112\,Pa,\quad T_0=260K$$

The temperature at wall is 242*K*. The station chosen for comparison has $c_f = 2.704\times10^{-3}$, and $q = 1.527\times10^{-3}$m.

The normal velocity profile is not an output in Wilcox's program. However, the normal velocity at the boundary layer edge (v_e) can be obtained from the integration of continuity equation using the solution of boundary layer equations at two adjacent stations. The value is found to be 0.6395m/s, and can be taken as a close approximate to the exact value. The corresponding value reproduced from the proposed procedure is 0.673m/s. It is remarkable that the difference is only about 5% of the exact value, considering the fact that v_e is only about 0.2% of the freestream velocity. The reproduced normal velocity profile is shown in Fig. 5. The comparison of the reproduced profiles for density, streamwise velocity, and temperature with the boundary layer solutions, is shown in Fig. 6. Comparison of skin friction coefficient, shape factor, and normal velocity at boundary layer edge is listed in Table 2.

A word of caution for the choice of streamwise step *Dx* in the integration of Eq. (12) is in order. It should neither be too large, to incur excessive discretization error, nor be too small, to incur round-off error. In the example above, non-dimensionalized *Dx* from 0.01 to 0.5 gave essentially the same results.

4. Specification of Turbulence Quantity Profiles

With the mean flow profiles of density, velocity, and temperature available, turbulent quantity profiles can be determined either from algebraic turbulence models, from experimentally established laws, or from their definitions in turbulence models.

1) Turbulent viscosity profile can be readily calculated with any simple algebraic turbulence model, say Baldwin-Lomax's model[26].
2) For the one-equation turbulence model of Spalart-Allmaras[27], the modeled quantity is related to the turbulent viscosity via an algebraic equation, hence can be determined from the solution of that equation.
3) For two-equation turbulence models[28,29,30], first the principal turbulence shear stress(τ_{xy}) is calculated as the product of the turbulent viscosity and the strain rate of the mean flow (neglecting velocity derivative along the flow direction). Then, turbulent kinetic energy k can be determined through the experimentally established relation[31] $\tau_{xy} = ak$, where a, the so-called structural parameter, has a value of about 0.3.
4) The turbulence dissipation rate (ε) or specific dissipation rate (w) can be deduced from k and turbulent viscosity according to their relationship in the turbulence models.
5) Within the viscous sublayer, there is no proportionality between (τ_{xy}) and k. Instead, asymptotic results from Taylor series expansion and Navier-Stokes equations applied in the vicinity of wall can be employed. The leading term of turbulent kinetic energy varies quadratically with the normal distance from the wall, the coefficient of which can be determined by matching the solutions in the near wall region with that in the region away from the wall. Analytical formula for specific dissipation rate (w) in the vicinity of wall exhibits an inversely quadratic behavior.

The profiles of turbulent viscosity (m_t), the quantity modeled in Spalart-Allmaras's one-equation turbulence model, turbulent kinetic energy (k), and specific turbulent dissipation rate (w), corresponding to the mean flow profiles in Fig. 6, are shown in Figs. 7-10, respectively.

5. Conclusions

The problem of specifying inflow profile boundary conditions involving compressible boundary layer is an area that has not received adequate attention. Huang et. al. modify the Van Driest I transformation to take into account the effect of realistic value of Pr_t, and apply it to the Coles' profile that is extended towards the viscous sublayer. They devise an iterative procedure to consistently determine skin friction coefficient and major mean flow profiles from given external flow conditions and boundary layer displacement or momentum thickness. In this paper, three modifications are proposed to make the iterative procedure more convenient and more accurate.

First, it is proposed to use Musker's explicit expression for the wall velocity distribution in place of the extended Coles's profile, which requires integration, to facilitate the iterative procedure.

Second, theoretical analysis shows that a new form of density-weighted velocity, rather the Van Driest density-weighted velocity, obeys the linear-law at the viscous sublayer in a compressible turbulent boundary layer. Especially

for nonadiabatic wall at hypersonic Mach numbers, where there are large density gradients, these two kinds of density-weighted velocity could differ considerably. The linear-law for the new kind of density-weighted velocity should be employed to modify the profiles at the sublayer.

Third, an iterative procedure is proposed for the case when boundary layer nominal thickness, rather than the displacement or momentum thickness, is given.

The effects of these modifications are checked against experimental results at hypersonic Mach number. Reasonable good agreement is obtained. It is also shown that power-law fitting for the streamwise velocity gives unacceptable profile in the viscous sublayer.

By incorporating continuity equation and integral momentum equation with the above iterative procedure, a way to determine normal velocity profile is proposed for the first time. The reproduced normal velocity at the boundary layer edge is found to agree remarkably well with the numerical solution of the boundary layer equations.

Besides the mean flow variable profiles, ways to set profiles for turbulent quantities, based on algebraic turbulence models and general experimental observations, are also proposed.

The same idea in this paper can be readily used in the determination of inflow profiles involving incompressible boundary layer.

References

(1). Thomas, J. L., and Salas, M. D., "Far Field Boundary Conditions for Transonic Lifting Solutions to the Euler Equations," *AIAA Journal*, Vol. 24, 1986, pp.1074-1080.

(2). Giles, M. B., "Nonreflecting Boundary Conditions for Euler Equation Calculations, " *AIAA Journal*, Vol. 28, No. 12, 1990, pp.2050-2058.

(3). Pulliam, T. H., and Steger, J. L., "Recent Improvements in Efficiency, Accuracy, and Convergence for Implicit Approximate Factorization Algorithms, " *AIAA Paper*-85-0360, 1985. AIAA 23rd Aerospace Sciences Meeting.

(4). Nordstrom, J., "Extrapolation Procedures for the Time-Dependent Navier-Stokes Equations, " *AIAA Journal*, Vol. 30, No. 6, 1992, pp.1654-1656.

(5). Rizzi, A. W., "Numerical Implementation of Solid-Body Boundary Conditions for the Euler Equations," ZAMM, Vol. 58, 1978, pp.301-304.

(6). Krist, S. L., Biedron, R. T., and Rumsey, C. L., "CFL3D User's Manual (Version 5.0)," NASA/TM-1998-208444. pp. 259-260.

(7). Orkwis, P. D., Tam, C. J., and Disimile P. J., "Observations on Using experimental Data as Boundary Conditions for Computations," *AIAA Journal*, Vol. 33, No. 1, 1995, pp.176-178.

(8). Zhang, X., "Compressible Cavity Flow Oscillation due to Shear Layer Instabilities and Pressure Feedback," *AIAA Journal*, Vol. 33, No. 8, 1995, pp. 1404-1411.

(9). Zhang, J. B., "Experimental and Computational Investigation of Supersonic Cavity Flows," Ph. D. Thesis, Dept. of Aeronautics and Astronautics, University of Tokyo, Japan, Sept. 2000, pp. 43-46.

(10). Spalding, D. B. and Chi, S. W., "The Drag of a Compressible Turbulent Boundary Layer on a Smooth Flat Plate With and Without Heat Transfer," *J. Fluid Mechanics*, Vol. 18, Pt. 1, Jan. 1964, pp. 117-143.

(11). Coles, D., "The Turbulent Boundary Layer in a Compressible Fluid," *The Physics of Fluids*, Vol. 7, No. 9, Sept. 1964.

(12). Van Driest, E. R., "Turbulent Boundary Layer in Compressible Fluids," *The Aeronautical Journal*, Vol.18, No. 3, 1951, pp. 145-160.

(13). Van Driest, E. R., " The Problem of Aerodynamic Heating," *Aeronautical Engineering Review*, Vol. 15, No. 10, Oct. 1956, pp. 26-41.

(14). Sommer, S. C. and Short, B. J., "Free-Flight Measurements of Turbulent-Boundary Layer Shin Friction in the Presence of Severe Aerodynamic Heating at Mach Numbers From 2.8 to 7.0", TN 3391, 1955, NACA.

(15). Baronti, P. O. and Libby, P. A., "Velocity Profiles in Turbulent Compressible Boundary Layers," *AIAA Journal*, Vol. 4, No. 2, 1966, pp.193-202.

(16). Huang, P. G., Bradshaw, P., and Coakley, T. J., "Skin Friction and Velocity Profile Family for Compressible Turbulent Boundary layers", *AIAA Journal*, Vol. 31, No. 9, 1993, pp1600-1604.

(17). Hopkins, E. J., and Inouye, M., "An Evaluation of Theories for Predicting Turbulent Skin Friction and Heat Transfer on Flat Plates at Supersonic and Hypersonic Mach Number, *AIAA Journal*, Vol. 9, No. 6, 1971, pp. 993-1003.

(18). Hopkins, E. J., Keener, E. R., Polek, T. E. and Dwyer, H. A., "Hypersonic Turbulent Skin-Friction and Boundary-Layer Profiles on Nonadiabatic Flat Plates," *AIAA Journal*, Vol. 10, No. 1, 1972, pp.40-48.

(19). Fernholz, H. H., and Finley, P. J., " A Critical Commentary on Mean Flow Data for Two-Dimensional Compressible Turbulent Boundary Layers," AGARD-AG-253, 1980.

(20). Cebeci, T., and Smith, A. M. O., *Analysis of Turbulent Boundary layers*, Academic Press, New York, 1974, p. 221.

(21). Musker, A. J., "Explicit Expression for the Smooth Wall Velocity Distribution in a Turbulent Boundary Layer", *AIAA Journal*, Vol. 17, No. 6, 1979, pp. 655-657.

(22). Cornish, J. J. III, " A Universal Description of Turbulent Boundary Layer Profiles With or Without Transpiration," Research Rept. 29, Mississippi State Univ., Aero Physics Dept., 1960.

(23). Bull, M. K., "Velocity Profiles of Turbulent Boundary Layers," *The Aeronautical Journal*, Vol.73, 1969, p. 143.

(24). Favre, A., "Equations des gaz turbulents compressibles," J. de Mecanique, Vol. 4., No. 3, 1965.

(25). Wilcox, D. C., "Turbulence Modeling for CFD", DCW Industries, Inc., La Canada, California, 1993.

(26). Baldwin, B. S., Lomax, H., Thin Layer Approximation and Algebraic Model for Separated Turbulent Flows, *AIAA Paper*-78-257, Jan. 1978.

(27). Spalart, P. R., Allmaras, S. R., A One-Equation Turbulence Model for Aerodynamic Flows, *AIAA Paper*-92-0439, 1992.

(28). Jones, W. P. and Launder, B. E.: The prediction of Laminarization with a Two-Equation Model of Turbulence. Int. J. Heat & Mass Transfer, vol. 15, no. 2, Feb. 1972, pp. 301-314.

(29). Wilcox, D. C., Reassessment of the Scale-Determining Equation for Advanced Turbulence Models, *AIAA Journal*, vol. 26, no. 11, 1988, pp.1299-1310.

(30). Menter F. R., Two-Equation Eddy-Viscosity Turbulence Models for Engineering Applications, *AIAA Journal*, vol. 32, no. 8, August 1994, pp.1598-1605.

(31). Townsend, A. A., *The Structure of Turbulent Shear Flow*, Second Edition, Cambridge University Press, Cambridge, 1976.

Table 1 Comparison of reproduced skin friction coefficient,
momentum and nominal thickness, and shape factor against the experimental values
(The figures in the parenthesis are the errors relative to the experiment)

	c_f	θ (cm)	δ (cm)	H
Given θ	8.0E-04(5.2%)		1.53(13.3%)	18.0(-4.2%)
Given δ	8.4E-04(10.5%)	0.0357(-23.0%)		18.1(-3.7%)
Experiment[18]	7.6E-04	0.0464	1.35	18.8

Table 2 Comparison of reproduced skin friction coefficient, shape factor
and normal velocity at the edge of boundary layer against the solution of BL eqns.
(The figures in the parenthesis are the errors relative to the BL solution)

	c_f	H	v_e (m/s)
Reproduced	2.66E-03(-1.5%)	1.68(-1.2%)	0.6730(5.2%)
Solution of BL eqns	2.70E-03	1.70	0.6395

Fig. 1 Comparison of reproduced streamwise velocity profiles with experiment values

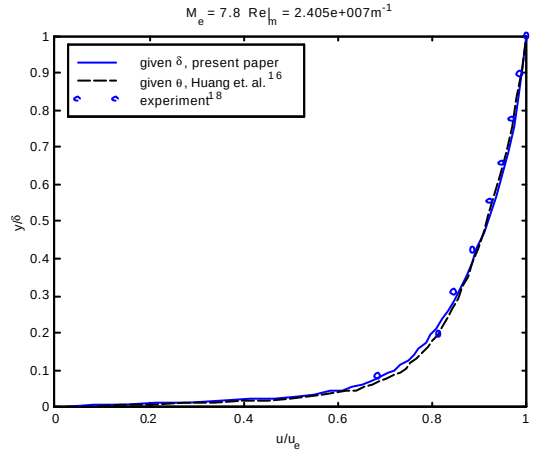

Fig. 2 Reproduced density and temperature profiles (Given θ)

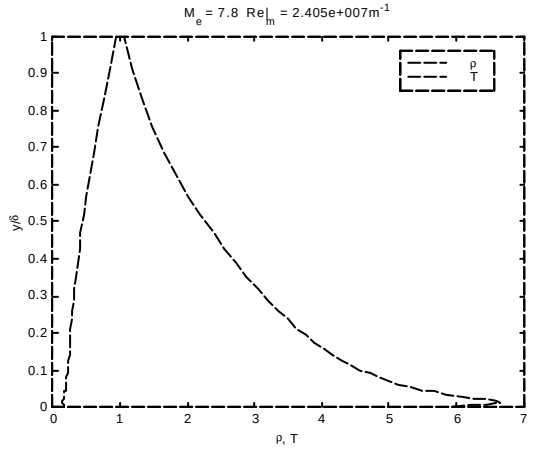

Fig. 3 Reproduced velocity distribution in viscous sublayer for hypersonic flow with iso-thermal wall.

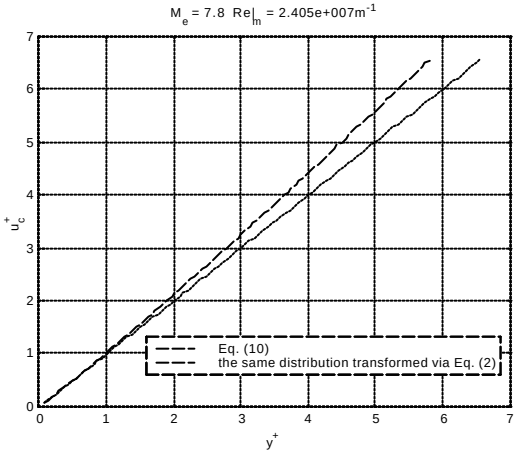

Fig. 4 Comparison of reproduced velocity profiles in wall unit between power-law and law-of-the-wall

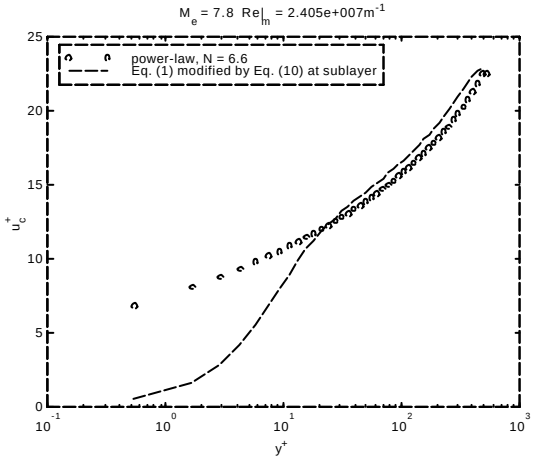

Fig. 5 Reproduced normal velocity profile

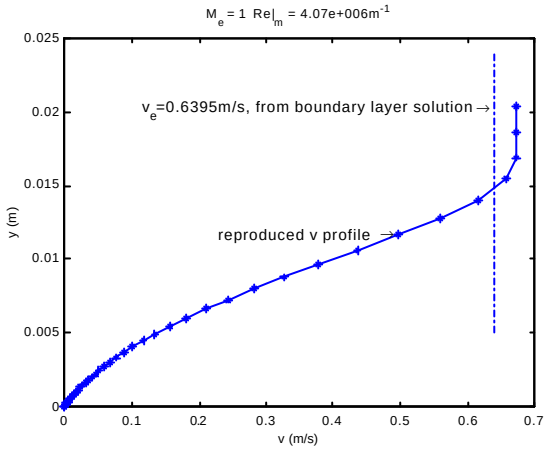

Fig. 6 Comparison of reproduced profiles and solution of boundary layer equations

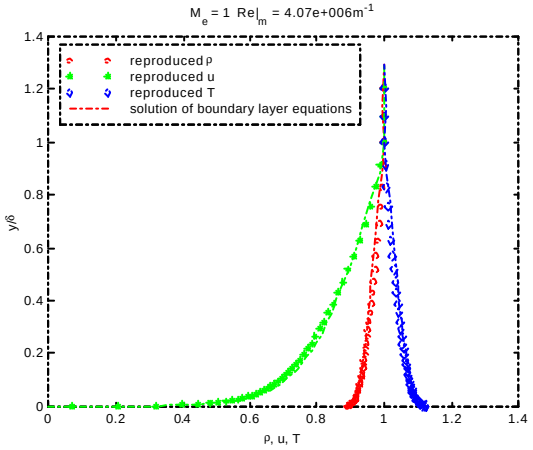

Fig. 7 Profiles of turbulent viscosity reproduced from Baldwin-Lomax algebraic turbulence models

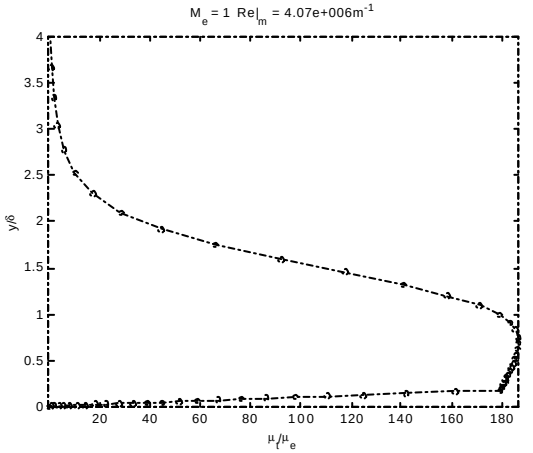

Fig. 8 Reproduced profile of the modeled quantity in Spalart-Allmaras's one-equation turbulence model

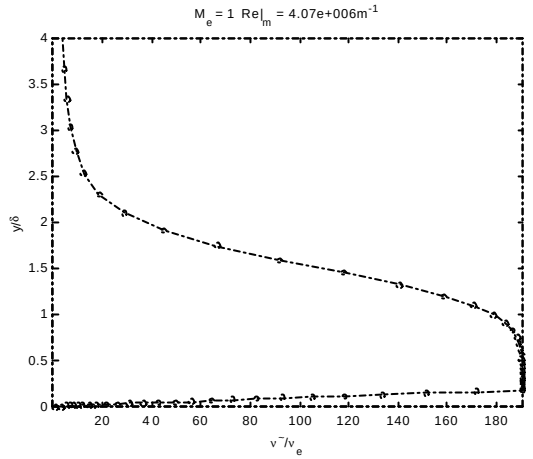

Fig. 9 Reproduced profile of turbulent kinetic energy

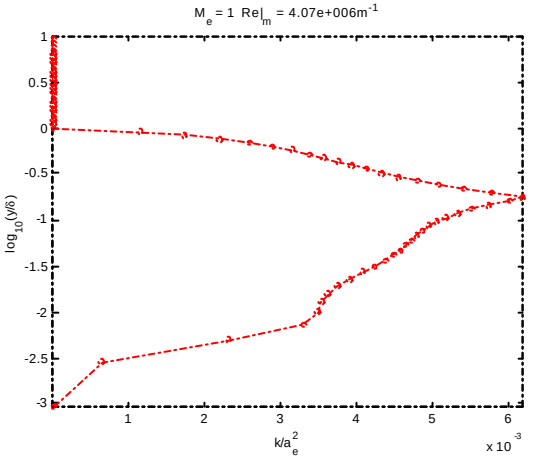

Fig. 10 Reproduced profile of turbulent specific dissipation rate